Measurement, direct numerical simulation and modelling of passive scalar transport in turbulent flows

by

Petra M. Wikström

December 1998
Technical Reports from
Royal Institute of Technology
Department of Mechanics
S-100 44 Stockholm, Sweden

Typsatt i LaTeX med Petra's *thesis-style*.

Akademisk avhandling som med tillstånd av Kungliga Tekniska Högskolan i Stockholm framlägges till offentlig granskning för avläggande av teknologie doktorsexamen torsdagen den 17 december 1998 kl 10.15 i Kollegiesalen, Administrationsbyggnaden, Kungliga Tekniska Högskolan, Valhallavägen 79, Stockholm.

Norstedts Tryckeri AB, Stockholm 1998

Measurement, direct numerical simulation and modelling of passive scalar transport in turbulent flows

Petra M. Wikström 1998
Department of Mechanics, Royal Institute of Technology
S-100 44 Stockholm, Sweden

Abstract

Passive scalar transport in turbulent flows is considered. The investigation is made both through physical and numerical experiments. Velocity and temperature measurements have been performed in the self-preserving region of a heated cylinder wake, for which the Reynolds number is higher than in earlier reported studies. The numerical experiments consist of a direct numerical simulation of a turbulent channel flow with an imposed mean scalar gradient. Also here the present Reynolds number is higher than those of earlier reported studies where spectral methods have been used. The present flow cases are used to extract and analyze features of importance for the mathematical modelling of scalar transport. The primary objective is to develop and analyze explicit algebraic models for the passive scalar flux.

An algebraic relation for the scalar flux, in terms of mean flow quantities, is formed by applying an equilibrium condition in the transport equations for the normalized scalar flux. This modelling approach is analogous to explicit algebraic Reynolds-stress modelling (EARSM) for the Reynolds-stress anisotropies. The assumption of negligible advection and diffusion of the normalized scalar flux gives in general an implicit, non-linear set of algebraic equations. A method for solving this implicit relation in a fully explicit form is proposed, where the term causing the non-linearity, *i.e.* the scalar production to dissipation ratio, is considered and solved for separately. The non-linearity, in the algebraic equations for the normalized scalar fluxes, may be eliminated directly by incorporating a non-linear term in the model of the pressure scalar-gradient correlation and the destruction and thus results in a much simpler model for both two- and three-dimensional mean flows. The proposed model of this type involves only one model parameter. The performance of this model is investigated in three different flow situations. These are homogeneous shear flow with an imposed mean scalar gradient, for which earlier published data are used, the turbulent channel flow with an imposed mean scalar gradient and the flow field downstream a heated cylinder. It is found to be possible to adjust the model parameter so that good agreement is achieved for the scalar fluxes in all these cases.

Descriptors: passive scalar, heated cylinder wake, turbulent channel flow, pressure scalar-gradient correlation, explicit algebraic modelling, shear flows, equilibrium, hot-wire anemometry, direct numerical simulations.

Preface

This thesis considers passive scalar transport in turbulent flows. The thesis is based on the following papers.

Paper 1. WIKSTRÖM, P. M., HALLBÄCK, M. & JOHANSSON, A. V. 1998 'Measurements and heat-flux transport modelling in a heated cylinder wake' *International Journal of Heat and Fluid Flow* **19**, 556-562.

Paper 2. WIKSTRÖM, P. M. & JOHANSSON, A. V. 1998 'DNS and scalar-flux transport modelling in a turbulent channel flow' In Proc. of *Turbulent Heat Transfer II*, pp. 6-46–6-51, May 31-June 5, Manchester, UK.

Paper 3. WIKSTRÖM, P. M., WALLIN, S. & JOHANSSON, A. V. 1998 'Derivation and investigation of a new explicit algebraic model for the passive scalar flux'. Submitted for publication.

Paper 4. WIKSTRÖM, P. M. & JOHANSSON, A. V. 1998 'On the modelling of the transport equation for the passive scalar dissipation rate' *4th International Symposium on Engineering Turbulence Modelling and Measurements*, May 24-26 1999, Corsica, France.

Paper 5. WIKSTRÖM, P. M. 1998 'Velocity and temperature measurements in the self-preserving region of a heated cylinder wake' TRITA-MEK, Technical Report 1998:9, Dept. of Mechanics, KTH, Stockholm, Sweden.

The papers are here re-set in the present thesis format, and some minor corrections have been made as compared to published versions.

Contents

CHAPTER 1

Introduction

The word turbulence has lately become a fashionable expression to characterize disorder and chaos in areas like politics and economy. A turbulent flow is also characterized by disorder in the sense that it contains eddies of many different sizes, giving a flow field that fluctuates rapidly in time and space. Due to its great wealth of complexity, turbulence is one of the most challenging problems in the field of classical physics. Some examples of turbulent flows are atmospheric flows, predicted in a weather forecast, the flow around an aircraft and the wake behind a submarine. In fact most flows in nature and engineering applications are turbulent. Consequently there is a large demand for improved understanding of turbulence and further development of different tools to predict turbulent flow.

The nature of turbulence is clearly demonstrated by the smoke from a cigarette which first moves straight upwards and then suddenly switches to a more swirling turbulent motion. This phenomenon provides a visualization of not only turbulence but also of the spreading of a passive scalar in a turbulent flow. The characteristic feature of a passive scalar is that its concentration is influenced by the turbulent motion, but does not itself influence the turbulent motion. In contrast an active scalar, like temperature in the combustion flow of your car engine, influences the turbulent velocity field quite strongly. In this case the fluid density is strongly affected by the temperature, whereas in the limit of passive scalar behaviour the induced density variations are negligible. Examples of passive scalar quantities are small amounts of heat, and pollutants in the atmospheric or ocean flows. The understanding and prediction of the transport of passive scalars in turbulent flows is not only important for the field of passive scalars itself, but may also be important in studies of cases with two-way interaction, such as buoyancy-driven flows. The modelling approaches often used for scalars in engineering applications like temperature in heat exchangers and species concentration in combustion flows are very similar to those of a passive scalar.

Another example of a visualization of a turbulent flow is the famous experiment of Osborne Reynolds in 1880. He studied the flow of water in a glass tube using ink as a passive marker. For low flow rates a steady streak of ink was seen throughout the tube, but for higher flow rates, “the colour band would all at once mix up with the surrounding water, and fill the rest of the tube with a mass of coloured water”. In 1883 he published a paper presenting the discovery of the important dimensionless number, *the Reynolds number*, quantifying the onset of turbulence. This was a major breakthrough in the field of fluid mechanics. Another important feature demonstrated, was that the mixing driven by turbulence is far more powerful than that due to fluctuations on a molecular level in a laminar flow.

During the first half of the nineteenth century Stokes, and Navier, worked with the equations describing the motion of the flow of a Newtonian fluid. It was in 1845 that these equations took the form that we today call the Navier-Stokes equations. These equations are non-linear and can not be solved analytically for turbulent flows. Today the Navier-Stokes equations may be solved numerically, using direct numerical simulations (DNS), for fully turbulent flows of moderate Reynolds numbers in simple geometries. See *e.g.* the land-mark paper of Kim *et al.* (1987). Due to the non-linearity there is a transfer of turbulent kinetic energy from larger scales to smaller scales, and this range of scales increases with increasing Reynolds number. The resulting computational workload increases approximately as the cube of the (macro-scale) Reynolds number. Despite the rapid development of computers, this still leads to rather severe restrictions on the range of Reynolds numbers tractable for this type of study. In many flow situations experiments are still the only alternative to resolve the large range of scales at high Reynolds numbers.

Historically, knowledge of the spreading of passive scalars in turbulent flows was gained experimentally in wind-tunnel measurements. Heat transfer in grid-generated isotropic and homogeneous turbulence was studied by Corrsin (1952), Warhaft & Lumley (1978), Tavoularis & Corrsin (1981), and Sirivat & Warhaft (1983). Among other things, the ratio of the thermal and dynamical timescales was investigated. The significance of this ratio in second-order modelling was discussed by Newman *et al.* (1981). Early studies of turbulent heat transfer in more complex geometries like the heated cylinder wake were made experimentally by *e.g.* Townsend (1949), Freymuth & Uberoi (1971) and LaRue & Libby (1974). On the request of Taylor (1932), pioneering measurements in the turbulent flow of a heated cylinder wake were made by Fage & Falkner, where mean velocity and mean temperature profiles were determined (see appendix of Taylor, (1932)).

Recently direct numerical simulation has become a more and more efficient tool in turbulence research. Pioneering direct numerical simulations of turbulent flows with imposed mean scalar gradients were performed by Rogers *et al.* (1986) in a homogeneous shear flow, and by Kim & Moin (1989) in a turbulent channel flow.

Statistical modelling of the Navier-Stokes equations, as well as of the conservation equation of a passive scalar, is a very efficient tool for prediction of high Reynolds number flows. Here variances and other single-point correlations are the quantities describing the turbulent field. The first scalar-flux models were much less sophisticated than many of those proposed today. The eddy-diffusivity hypothesis, *i.e.* gradient-diffusion model, for the mean turbulent scalar fluxes was used by Prandtl (1910). He assumed a constant turbulent Prandtl number, *i.e.* the ratio of the eddy viscosity and the eddy diffusivity. This constant was taken to be unity, which implies equal turbulent diffusivities of heat and momentum. The existence of an analogy between heat and momentum transfer in a fluid was first proposed by Reynolds (1874) as discussed by von Kármán (1939).

In later studies the two-equation model approach for passive scalars has been developed, thus allowing variations of the turbulent Prandtl number. A tensor eddy diffusivity proportional to the Reynolds stresses was introduced by Daly & Harlow (1970). Using a tensor eddy diffusivity the scalar fluxes are in general not assumed to be aligned with the mean scalar gradient. In the seventies a large effort began to be put into the development of transport-equation models for the scalar fluxes. This level of modelling, which is much more sophisticated than the eddy-diffusivity approach, includes modelling the pressure scalar-gradient correlation appearing in the transport equation for the scalar fluxes. The modelling of this term was studied early on by *e.g.* Launder (1975) who also introduced the inclusion of rapid terms in this modelling. Recently there has been a large interest in developing algebraic scalar-flux models obtained from the transport equations using some equilibrium assumption equivalent to that introduced by Rodi (1972) and (1976). The explicit forms of these models are particularly attractive since they lead to fewer numerical problems and reduced computational efforts compared to transport-equation modelling.

This thesis is a study of passive scalar transport in turbulent flows. The investigation is performed both through experiments and direct numerical simulations. The measurements are made in a heated cylinder wake at a Reynolds number higher than in previously reported experimental studies of this flow. The direct numerical simulation is a study of turbulent channel flow with an imposed mean scalar gradient. It has been carried out using spectral methods at the highest reported Reynolds number to date in its category.

The investigated flow cases are used for analysis and development of statistical modelling of passive scalar flux. A new explicit algebraic scalar-flux model, with a fairly simple formulation, is proposed together with a thorough analysis of the modelling of the pressure scalar-gradient correlation.

CHAPTER 2

Basic equations

2.1. The velocity field

The governing equations for an incompressible turbulent flow of a viscous fluid are the Navier-Stokes equations and the continuity equation given by

$$\frac{\partial U_i'}{\partial t} + U_l' \frac{\partial U_i'}{\partial x_l} = -\frac{1}{\rho}\frac{\partial P'}{\partial x_i} + \nu \frac{\partial^2 U_i'}{\partial x_l \partial x_l} \tag{1a}$$

$$\frac{\partial U_i'}{\partial x_i} = 0 \tag{1b}$$

where U_i' is the total velocity field, P' is the total modified pressure (which may contain a gravitational potential), and ρ and ν are the density and kinematic viscosity of the fluid respectively. The Reynolds decomposition $U_i' = U_i + u_i$, $P_i' = P + p$, where U_i and u_i are the mean and fluctuating parts of the velocity field and P and p are the mean and fluctuating parts of the pressure field, is applied here. In statistically stationary turbulence the mean value of a flow variable can be taken as the time average. Generally an averaged quantity is the ensemble average over an infinite number of realizations. By inserting these decompositions into the Navier-Stokes equations and taking the ensemble average, the Reynolds averaged Navier-Stokes equations (RANS) are obtained

$$\frac{\partial U_i}{\partial t} + U_l \frac{\partial U_i}{\partial x_l} = -\frac{1}{\rho}\frac{\partial P}{\partial x_i} + \frac{\partial}{\partial x_l}\left(\nu \frac{\partial U_i}{\partial x_l} - \overline{u_i u_l}\right) \tag{2a}$$

$$\frac{\partial U_i}{\partial x_i} = 0 \tag{2b}$$

The quantity $-\rho\overline{u_i u_l}$ is known as the Reynolds stress tensor and originates from the non-linear advective term of (1a). It is due to this term that the so called closure problem arises. This means that it is not possible to obtain a closed set of equations, since every new introduced transport equation will contain higher-order moments of the turbulent field.

The transport equations for the Reynolds stresses are given by

$$\begin{aligned}\frac{\mathrm{D}\overline{u_i u_j}}{\mathrm{D}t} = &-\overline{u_i u_l}\frac{\partial U_j}{\partial x_l} - \overline{u_j u_l}\frac{\partial U_i}{\partial x_l} + \overline{\frac{p}{\rho}\left(\frac{\partial u_i}{\partial x_j} + \frac{\partial u_j}{\partial x_i}\right)} - 2\nu\overline{\frac{\partial u_i}{\partial x_l}\frac{\partial u_j}{\partial x_l}} \\ &- \frac{\partial}{\partial x_l}\left(\overline{u_i u_j u_l} + \overline{\frac{p}{\rho}\left(u_i\delta_{jl} + u_j\delta_{il}\right)} - \nu\frac{\partial}{\partial x_l}\left(\overline{u_i u_j}\right)\right),\end{aligned} \tag{3}$$

where the operator

$$\frac{\mathrm{D}}{\mathrm{D}t} = \frac{\partial}{\partial t} + U_l \frac{\partial}{\partial x_l} \tag{4}$$

denotes the rate of change in a coordinate system following the mean velocity field. The first two terms on the right hand side of (3) are production due to mean field gradients. The next two terms are the traceless pressure-strain correlation and viscous destruction (or the 'homogeneous' dissipation rate). The last term is a diffusion term containing both turbulent and molecular diffusion. The first two terms inside the parenthesis of the diffusion term is the turbulent transport flux and the divergence of this flux is the rate of spatial redistribution among the different Reynolds stress components due to inhomogeneities in the flow field.

The transport equation for the kinetic energy, $K \equiv \frac{1}{2}\overline{u_i u_i}$, is

$$\frac{\mathrm{D}K}{\mathrm{D}t} = \mathcal{P}_K - \varepsilon + D^{(K)}, \tag{5}$$

where

$$\mathcal{P}_K = -\overline{u_i u_l}\frac{\partial U_i}{\partial x_l}, \qquad \text{and} \qquad \varepsilon = -\nu\overline{\frac{\partial u_i}{\partial x_l}\frac{\partial u_i}{\partial x_l}}. \tag{6}$$

The quantity $\mathcal{P}_K$ is the turbulent energy production, which describes the energy transfer between the mean and the fluctuating velocity fields, and ε is the 'homogeneous' dissipation rate of K. The quantity $D^{(K)}$, given by

$$D^{(K)} = \frac{\partial}{\partial x_l}\left(\nu \frac{\partial K}{\partial x_l} - \frac{1}{2}\overline{u_i u_i u_l} - \overline{\frac{p}{\rho} u_l}\right), \tag{7}$$

is the sum of molecular and turbulent diffusion of K. The transport equation for the dissipation rate ε is given by

$$\begin{aligned}
\frac{\mathrm{D}\varepsilon}{\mathrm{D}t} =& \frac{\partial}{\partial x_j}\left(\nu\frac{\partial \varepsilon}{\partial x_j} - \overline{u_j \varepsilon'} - 2\frac{\nu}{\rho}\overline{\frac{\partial p}{\partial x_k}\frac{\partial u_j}{\partial x_k}}\right) - 2\nu\overline{\frac{\partial u_i}{\partial x_j}\frac{\partial u_i}{\partial x_k}\frac{\partial u_j}{\partial x_k}} - 2\nu\overline{\frac{\partial u_i}{\partial x_k}\frac{\partial u_j}{\partial x_k}}\frac{\partial U_i}{\partial x_j} \\
&- 2\nu\overline{\frac{\partial u_k}{\partial x_i}\frac{\partial u_k}{\partial x_j}}\frac{\partial U_i}{\partial x_j} - 2\nu\,\overline{u_k\frac{\partial u_i}{\partial x_j}}\frac{\partial^2 U_i}{\partial x_j \partial x_k} - 2\nu^2\overline{\frac{\partial^2 u_i}{\partial x_j \partial x_k}\frac{\partial^2 u_i}{\partial x_j \partial x_k}},
\end{aligned} \tag{8}$$

where $\varepsilon' = \nu\frac{\partial u_i}{\partial x_l}\frac{\partial u_i}{\partial x_l}$. The first term on the right hand side of (8) consists of molecular and turbulent diffusion. The second term is a turbulent production term which represents stretching of the velocity field through the fluctuating velocity gradients (vortex stretching). The three following terms are mean gradient production terms and the last term is a viscous destruction term.

2.2. The scalar field

The governing equations for a passive scalar have many similarities to those of the velocity field of an incompressible flow of a viscous fluid. The conservation equation of a passive scalar is given by

$$\frac{\partial \Theta'}{\partial t} + U_l' \frac{\partial \Theta'}{\partial x_l} = \alpha \frac{\partial^2 \Theta'}{\partial x_l \partial x_l}, \tag{9}$$

where α is the molecular diffusivity. It is very similar to (1a) except for the pressure term. There is thus no direct coupling between the scalar field and the pressure field. For the passive scalar the coupling to the pressure field comes through the velocity field.

In analogy with the Reynolds decomposition of the velocity field the instantaneous scalar field may be divided into a mean part and a fluctuating part, $\Theta' = \Theta + \theta$. The transport equation of the mean scalar is obtained by inserting this decomposition into (9) and taking the ensemble average, which then gives

$$\frac{\partial \Theta}{\partial t} + U_l \frac{\partial \Theta}{\partial x_l} = \frac{\partial}{\partial x_l}\left(\alpha \frac{\partial \Theta}{\partial x_l} - \overline{u_l \theta} \right). \tag{10}$$

The scalar-flux term, $\overline{u_i \theta}$, or Reynolds-flux term in analogy with the Reynolds stress, is due to the non-linear advection term in (9) and leaves (10) unclosed. The transport equation for the scalar flux is given by

$$\begin{aligned}\frac{\mathrm{D}\overline{u_i\theta}}{\mathrm{D}t} = &- \overline{u_i u_l}\frac{\partial \Theta}{\partial x_l} - \overline{u_l\theta}\frac{\partial U_i}{\partial x_l} + \overline{\frac{p}{\rho}\frac{\partial \theta}{\partial x_i}} - (\alpha+\nu)\overline{\frac{\partial \theta}{\partial x_l}\frac{\partial u_i}{\partial x_l}} \\ &- \frac{\partial}{\partial x_l}\left(\overline{u_i u_l \theta} + \overline{\frac{p}{\rho}\theta}\delta_{il} - \alpha\overline{\frac{\partial \theta}{\partial x_l}u_i} - \nu\overline{\theta\frac{\partial u_i}{\partial x_l}}\right),\end{aligned} \tag{11}$$

which is similar to that for the Reynolds stresses. The right hand side of the transport equation (11) contains two production terms due to mean field gradients, a pressure scalar-gradient correlation term, viscous and diffusive destruction and a transport term consisting of turbulent and molecular diffusion.

The transport equation for half the scalar variance, $K_\theta \equiv \frac{1}{2}\overline{\theta^2}$, a quantity corresponding to the turbulent kinetic energy, is obtained by multiplying (9) with the fluctuating scalar θ and then taking the ensemble average of the resulting equation. This yields

$$\frac{\mathrm{D}K_\theta}{\mathrm{D}t} = \mathcal{P}_\theta - \varepsilon_\theta + D^{(K_\theta)}, \tag{12}$$

where

$$\mathcal{P}_\theta = -\overline{u_i\theta}\frac{\partial \Theta}{\partial x_i}, \qquad \text{and} \qquad \varepsilon_\theta = \alpha\overline{\frac{\partial \theta}{\partial x_k}\frac{\partial \theta}{\partial x_k}} \tag{13}$$

are the production, which is due to the mean scalar gradient, and the dissipation rate of K_θ. The quantity $D^{(K_\theta)}$, which is the sum of molecular and turbulent diffusion of K_θ, is given by

$$D^{(K_\theta)} = \frac{\partial}{\partial x_j}\left(\alpha \frac{\partial K_\theta}{\partial x_j} - \frac{1}{2}\overline{u_j \theta^2} \right) \tag{14}$$

As in the previous equations for the scalar field the transport equation for the scalar dissipation rate ε_θ contains terms which are quite similar to those in the corresponding transport equation for the velocity field. It reads

$$\begin{aligned}\frac{\mathrm{D}\varepsilon_\theta}{\mathrm{Dt}} =& \frac{\partial}{\partial x_j}\left(\alpha\frac{\partial \varepsilon_\theta}{\partial x_j} - \overline{u_j\varepsilon'_\theta}\right) - 2\alpha\,\overline{\frac{\partial u_j}{\partial x_k}\frac{\partial \theta}{\partial x_k}\frac{\partial \theta}{\partial x_j}} - 2\alpha\,\overline{\frac{\partial u_j}{\partial x_k}\frac{\partial \theta}{\partial x_k}}\frac{\partial \Theta}{\partial x_j}\\ &- 2\alpha\,\overline{\frac{\partial \theta}{\partial x_j}\frac{\partial \theta}{\partial x_k}}\frac{\partial U_j}{\partial x_k} - 2\alpha\,\overline{u_j\frac{\partial \theta}{\partial x_k}}\frac{\partial^2 \Theta}{\partial x_k \partial x_j} - 2\alpha^2\,\overline{\left(\frac{\partial^2 \theta}{\partial x_j \partial x_k}\right)^2}, \qquad (15)\end{aligned}$$

where $\varepsilon'_\theta = \alpha\frac{\partial\theta}{\partial x_k}\frac{\partial\theta}{\partial x_k}$. The first term on the right hand side of (15) consists of molecular and turbulent diffusion. The second term is a turbulent production term which represents stretching of the scalar field through the fluctuating velocity gradients. The three following terms are mean gradient production terms and the last term is a diffusive destruction term.

2.3. Different levels of modelling

The objective of scalar-flux modelling is to close equation (10). This closure may for example be a simple eddy-diffusivity hypothesis, in analogy with the eddy-viscosity hypothesis for the Reynolds stresses, or may consist of several additional transport equations. The modelling level for the Reynolds fluxes should not be higher than that of the Reynolds stresses, since the scalar transport predictions rely heavily on the velocity field description (including its turbulence statistics, see So *et al.* [44]). In the following different levels in the hierarchy of modelling of passive scalar flux are discussed.

2.3.1. Transport equation modelling. In transport-equation modelling, of the passive scalar flux, the transport equations for K_θ, its destruction rate, ε_θ, and the passive scalar flux, $\overline{u_i\theta}$, are modelled. The model for the scalar fluxes is then of the form

$$\frac{\mathrm{D}\overline{u_i\theta}}{\mathrm{D}t} = F_i^{(\mathrm{TRANS})}\left(\overline{u_m u_n}, \frac{\partial U_m}{\partial x_n}, \overline{u_m\theta}, \frac{\partial \Theta}{\partial x_m}, K, K_\theta, \varepsilon, \varepsilon_\theta\right) \qquad (16)$$

The first two, K_θ, ε_θ, are needed to estimate the decay-timescale ratio, $r \equiv K_\theta\varepsilon/K\varepsilon_\theta$, for the passive scalar. Information about the scalar timescale, $K_\theta/\varepsilon_\theta$, may be particularly important in situations where it differs significantly from the dynamical timescale K/ε. The set of transport equations is solved together with modelled transport equations for the Reynolds stresses, or $\overline{u_iu_j}$, and the dissipation rate of the turbulent kinetic energy, ε. This level of modelling captures a large part of the relevant phenomena involved in engineering flows, but leads in complicated geometries with three-dimensional mean flows to sixteen transport equations. Of these equations six are from the scalar field; (10), (11) (*i.e.* three equations), (12) and (15).

The transport equation (11) for the scalar flux may be written in symbolic form as

$$\frac{\mathrm{D}\overline{u_i\theta}}{\mathrm{Dt}} = \mathcal{P}_{\theta i} + \Pi_{\theta i} - \varepsilon_{\theta i} + D_i, \tag{17}$$

where $\mathcal{P}_{\theta i}$, $\Pi_{\theta i}$, $\varepsilon_{\theta i}$, and D_i are the production, pressure scalar-gradient correlation, destruction and diffusion terms respectively. Here it is seen that the construction of the relation (16) involves modelling of the pressure scalar-gradient correlation and the molecular destruction terms, as well as the the turbulent diffusion terms. Several models for the pressure scalar-gradient correlation (often also including the destruction term) have been reported in the literature. Since the pressure itself may be divided into a slow and a rapid part this is also the case for $\Pi_{\theta i}$. From the Poisson equation for the pressure it may be seen that the rapid terms involve the mean velocity gradients linearly, see *e.g.* Shih [41] and Launder [25]. The model of Launder [24], which contains both a rapid and a slow term, is

$$\Pi_{\theta i} = -c_{\theta 1}\frac{1}{\tau}\overline{u_i\theta} + c_{\theta 2}\overline{u_j\theta}\frac{\partial U_i}{\partial x_j}, \tag{18}$$

where the timescale τ was taken as the dynamical timescale (in Launder [25] it was suggested that both the dynamical and thermal timescales are important) and the model parameters $c_{\theta 1}$ and $c_{\theta 2}$ were assigned constant values of 3.2 and 0.5 respectively. In the model of Rogers *et al.* [38] only the slow part, *i.e.* the $c_{\theta 1}$ term, was included, whereas a Reynolds number and a Prandtl number dependence was included in the $c_{\theta 1}$ parameter. Several additional terms for both the slow and rapid parts are included in the models of Craft & Launder [8] (14 terms) and [9] (12 terms). A model commonly adopted for the diffusion term is the gradient-diffusion model proposed by Daly & Harlow [10], which is given by

$$D_i = \frac{\partial}{\partial x_k}\left(c_\theta \frac{k}{\varepsilon}\overline{u_k u_l}\frac{\partial \overline{u_i\theta}}{\partial x_l}\right). \tag{19}$$

The modelling of the pressure scalar-gradient correlation and the molecular destruction terms is investigated in Paper 1 [54], Paper 2 [55] and Paper 3 [56], and modelling of the turbulent diffusion terms, is briefly investigated in Paper 1.

2.3.2. Explicit algebraic scalar-flux modelling. Through approximation of the modelled transport equation of the scalar flux an algebraic scalar-flux model, that still contains a considerable part of the underlying physics, may be obtained. There is a great interest in algebraic scalar-flux models which are obtained from the transport equations using some equilibrium assumption equivalent to that used to formulate algebraic Reynolds-stress models (ARSM), see *e.g.* Adumitroaie *et al.* [3], Girimaji & Balachandar [14], Abe *et al.* [2], Shabany & Durbin [40], Shih & Lumley [42] and Shih [41]. The scalar-flux model is then of the form

$$\overline{u_i\theta} = F_i^{(\mathrm{ARFM})}\left(\overline{u_m u_n}, \frac{\partial U_m}{\partial x_n}, \overline{u_m\theta}, \frac{\partial \Theta}{\partial x_m}, K, K_\theta, \varepsilon, \varepsilon_\theta\right). \tag{20}$$

The equilibrium assumption excludes the diffusion terms, whereas models of the pressure scalar-gradient correlation and molecular destruction terms are still needed, just as in transport-equation modelling. The explicit forms of these algebraic models are attractive since they lead to fewer numerical problems and reduced computational efforts compared to full second-order closures. To be able to construct explicit forms, the model for the pressure scalar-gradient correlation and the destruction, $\Pi_{\theta i} - \varepsilon_{\theta i}$, has to be linear in the scalar-flux except for a non-linearity identical to that appearing when applying the equilibrium assumption to the transport equation for the normalized scalar fluxes, see Chapter 5 and Paper 3. An EARFM can be written in the following symbolic form

$$\overline{u_i\theta} = F_i^{(\mathrm{EARFM})}\left(\overline{u_m u_n}, \frac{\partial U_m}{\partial x_n}, \frac{\partial \Theta}{\partial x_m}, K, K_\theta, \varepsilon, \varepsilon_\theta\right). \tag{21}$$

In Paper 3 a new explicit algebraic Reynolds-flux model is presented. The modelling approach for the Reynolds fluxes, $\overline{u_i\theta}$, is analogous to that of an EARSM (explicit algebraic Reynolds-stress model) for the Reynolds stresses, see *e.g.* Wallin & Johansson, [50] and [51], Gatski & Speziale [13] or Taulbee [46]. In Chapter 5 explicit algebraic modelling is discussed in more detail together with a presentation of the EARFM of Paper 3.

2.3.3. Eddy-diffusivity models. In an eddy-diffusivity model for the passive scalar field the the scalar fluxes are approximated by

$$\overline{u_i\theta} = -\alpha_t \frac{\partial \Theta}{\partial x_i}, \tag{22}$$

where α_t is the eddy diffusivity. This is analogous to the classical Boussinesq approximation or eddy-viscosity hypothesis for the Reynolds stresses,

$$\overline{u_i u_j} = -\nu_t \left(\frac{\partial U_i}{\partial x_j} + \frac{\partial U_j}{\partial x_i}\right) + \frac{2}{3}K\delta_{ij}, \tag{23}$$

where ν_t is the eddy viscosity. In a two-equation level of modelling the eddy diffusivity is obtained from

$$\alpha_t = \frac{\nu_t}{Pr_t(r)}, \tag{24}$$

where the turbulent Prandtl number (or Schmidt number) can be modelled as a function of the timescale ratio, r. At this level of modelling it is therefore necessary to solve for the equations for K_θ and ε_θ. Significant progress in this type of modelling has been made by *e.g.*, Nagano & Kim [28], Nagano *et al.* [29], Yossef *et al.* [59] and Abe *et al.* [1].

At a zero-equation level of modelling the turbulent Prandtl number, or equivalently the timescale ratio, r, is assumed to be constant and no further equations are needed. A computation of flow and heat transfer through rotating ribbed passages was recently made by Iacovides [15] using a zero-equation model for the heat fluxes combined with a two-equation eddy-viscosity model and a transport-equation model for the Reynolds stresses.

Whether it is a two-equation model or a zero-equation model, the eddy diffusivity approach, using a scalar eddy diffusivity, is unable to always predict realistic values of all components of $\overline{u_i\theta}$, since it assumes that the scalar flux is aligned with the mean scalar gradient. See for example Wikström *et. al* [53] and Paper 5 [58], where the streamwise heat flux, $\overline{u\theta}$, in the heated cylinder wake then is predicted to be zero. In reality, $\overline{u\theta}$, and the cross-stream heat flux, $\overline{v\theta}$, are both non-zero and of the same magnitude.

CHAPTER 3

Measurements in a heated cylinder wake

In this study the flow behind an electrically heated circular cylinder, placed horizontally in a wind tunnel, is considered. The cylinder length to diameter ratio is high enough for the flow to be considered two-dimensional. Also, the velocity is high enough and the heating is low enough for buoyancy effects to be negligible. A sketch of the resulting flow situation is presented in Fig. 3.1. The velocity deficit, U_s, and the temperature excess, Θ_s, at the centerline, decrease in the streamwise direction, whereas the mean velocity-defect half width, l, increases. The wake profiles thus spread out in the cross-stream direction with increasing distance from the cylinder. The temperature fluctuations are convected downstream along a mean stream line. These fluctuations are produced due to flow instabilities, decay due to thermal dissipation and redistributed by diffusion.

The flow behind a heated circular cylinder has been studied experimentally by several investigators previously. The pioneering work of Townsend (1949) included measurements of transport of heat at different downstream positions. With the evolution of digital computers in the seventies, as well as the improvement of experimental techniques, experiments became a more efficient tool to analyze turbulent flows. Thorough investigations of the heated cylinder wake were made experimentally by Freymuth & Uberoi [12], Fabris [11] and Browne & Antonia [6] and Antonia & Browne [4]. The Reynolds number based on the freestream velocity and the cylinder diameter, and the downstream position, (Re, x/d), were (960,1140) in the measurements of Freymuth & Uberoi, (2700,400) in those of Fabris, and (1170,420) in the experiments by Browne & Antonia and Antonia & Browne, respectively.

The concept of self-similarity is very useful when analyzing turbulent shear flows like wakes, jets and mixing layers. This means that the evolution of the flow may be determined using only local scales of length and velocity. In the experiments by Townsend [49] the normal stresses and the shear stresses were found to reach a self-similar state for x/d of approximately 500 and larger. In later work self-similarity has been found to prevail at somewhat smaller distances from the cylinder. Freymuth & Uberoi [12] found the distributions of mean and fluctuating temperatures to be self-similar for x/d larger than approximately 100, and in the experiments by Aronson and Löfdahl [5] the distributions of the mean velocity and Reynolds stresses were self-similar for x/d of about 200 and more.

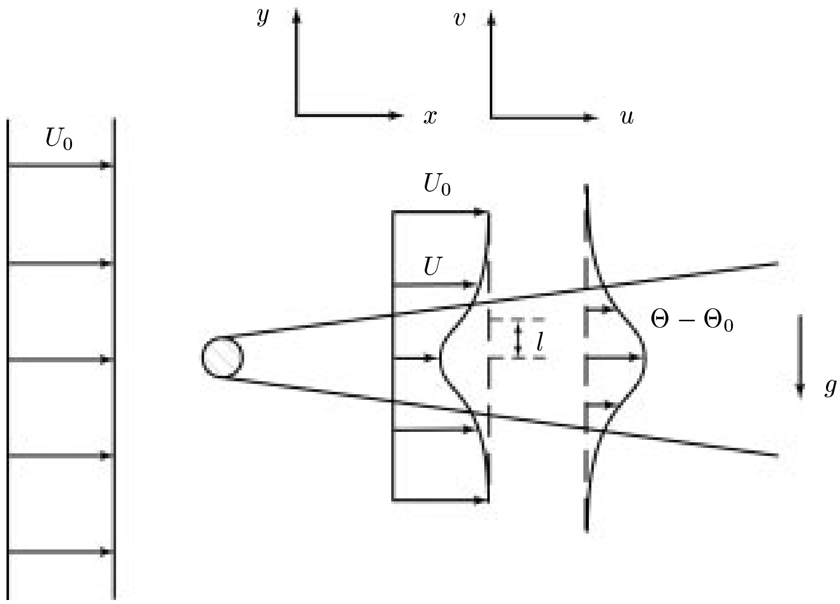

FIGURE 3.1 The mean velocity and mean temperature profiles in a wake behind a heated circular cylinder, where $U_s = U_0 - U_{\min}$, $\Theta_s = \Theta_{\max} - \Theta_0$ and l is the mean velocity-deficit half width.

3.1. Experimental procedure

The MTL wind tunnel, at KTH, Stockholm, with a 7.0 m long test section of 1.2×0.8 m^2 cross section and a free stream turbulence level less than 0.05% was used in the experiments. A picture of the MTL wind tunnel is given in Fig. 3.2. The diameter of the horizontal wake-generating cylinder was 6.4 mm and all the measurements were made at a velocity, U_0, of 10.1 m/s giving a maximum mean velocity deficit of 0.5 m/s at $x/d = 400$. The present Reynolds number, $U_0 d/\nu = 4300$, is about three times higher than that of Browne & Antonia [6]. The cylinder was electrically heated giving a maximum mean temperature excess, Θ_s, of 0.8 $^\circ C$ above the ambient air temperature at $x/d = 400$. Measurements were made at the following four different downstream positions: $x/d = 200$, 400, 600 and 800.

Simultaneous measurements of velocity and temperature statistics were made using a three-wire probe configuration (in-house construction) consisting of an X-probe, with platinum wire sensors, for velocity measurements and a single cold platinum wire for temperature measurements, located 0.5 mm in front of the X-wire mid point. The hot wires had a length of 0.5 mm and a diameter of

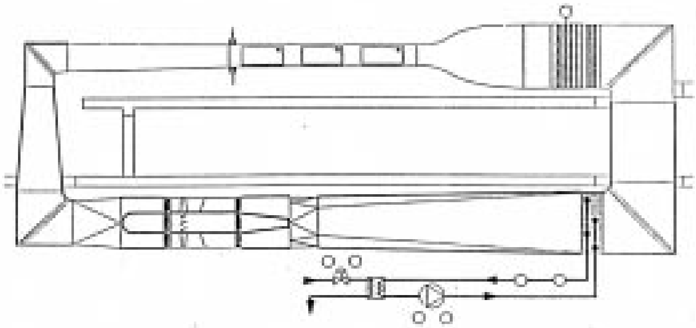

FIGURE 3.2 The MTL wind tunnel circuit.

2.5 μm and were operated with an overheat ratio of about 50%. The corresponding dimensions for the cold wire were 1.0 mm and 0.63 μm and it was operated at a constant current of 0.3 mA. This current is low enough to ensure negligible overheating of the wire thereby ensuring negligible sensitivity to velocity fluctuations. As analyzed in Paper 5, the length to diameter ratio of cold wires needs to be several times larger than typical values used for hot-wires. These ratios are here chosen to be about 1600 and 200, respectively.

An angular calibration procedure, using a Pitot tube, was carried out for the X-probe. Third order polynomials were fitted to the calibration data, covering the range of velocities and flow angles occurring during measurements in the wake. The cold wire was calibrated against an NTC-resistor (a thermistor) using 4 different heatings of the cylinder, giving a temperature span of about 1 $°C$.

During measurements the probe was traversed by an automated procedure controlling the traversing system. At each point $3\times1024\times200$ samples of voltages from the constant temperature and constant current circuits were filtered at 5 kHz and sampled at 10 kHz. The data were then saved on a CD-Recordable disc for later postprocessing.

Cross-stream derivatives of measured quantities were obtained by using cubic-spline smoothing of the data. Derivatives in the streamwise direction, needed to determine advective terms, were obtained by assuming self-similarity.

3.2. Results

The streamwise variations of the maximum velocity defect, U_s, the maximum temperature excess, Θ_s, and the velocity-defect half-width, l, are in good agreement with those of Browne & Antonia [6], (Wikström et al. [53] and Paper 5). The distributions of mean velocity and mean temperature reach self-similarity at about $x/d = 200$, while second-order moments, like $\overline{uv}$ and $\overline{v\theta}$, reach self-similarity at an x/d of approximately 400.

In Paper 1 budgets for the scalar fluxes are presented. Here it is found that the pressure scalar-gradient correlation is as large as the production terms. Estimates of the destruction terms indicate that these are quite small compared to the pressure scalar-gradient correlation. This is in agreement with the DNS data of Overholt & Pope [31], for which the destruction terms in the scalar-flux budget are shown to be negligible at high enough Reynolds numbers. The turbulent diffusion terms are significant in the present wake flow, whereas the molecular diffusion terms are negligible.

In Paper 1 and Paper 3 the modelling of the sum of the pressure scalar-gradient correlation and the destruction terms is analyzed using the present experimental data. It is found that it is important to include a mixture of both the thermal timescale, $K_\theta/\varepsilon_\theta$, and the dynamical timescale, K/ε, in the modelling of the slow part. The timescale ratio, r, shows a quite large variation through the wake. An assumption of a constant r or a turbulent Prandtl number, Pr_t, is thus not appropriate here.

The influence of rapid terms is studied in Paper 1, where a clear influence of these terms is found. In a more general context it is found difficult to obtain a modelling of the rapid part that can give an improvement in a wide class of flows. By using the test cases of homogeneous turbulent shear flow, channel flow and the heated cylinder wake it can be concluded that a more primary influence is that of the timescale ratio, and to some extent the mean temperature gradient on the coefficient of the 'slow' term (see Paper 3).

In Paper 1 modelling of the triple correlations $\overline{u_i u_j \theta}$ is also investigated. These are needed to determine the turbulent diffusion term in the transport equation of the scalar fluxes. Here it is found that when using the truncated Shih [41] model, only two of the terms may give approximately as good predictions as those of a model including all nine terms. When only using a Daly & Harlow type gradient-diffusion model, the $\overline{w^2\theta}$ component may not be captured in the present flow case.

The scalar fluxes are presented in Chapter 5 and the heated cylinder wake is one of the test cases for the explicit algebraic Reynolds-flux model presented in Paper 3 and (more briefly) in Chapter 5.

CHAPTER 4

DNS of a turbulent channel flow

Direct numerical simulations of plane turbulent channel flows with imposed mean scalar gradients have been performed by several investigators previously. In the simulations of Kim & Moin [22] the Reynolds number, Re_τ, based on the friction velocity, u_τ, and the channel half width, δ, is 180 and the Prandtl numbers used are 0.1, 0.71 and 2. Two different types of boundary conditions are studied. In the first case the scalar is generated internally and removed from isothermal walls with the same temperature (or scalar concentration). For the second case the isothermal boundary condition is applied with walls of different temperature, which means that the passive scalar is introduced at one wall and removed from the other. Profiles of the mean scalar, the scalar variance and the scalar fluxes are presented for the first case, while for the latter case data is presented through studies of turbulent structures for the scalar field.

Kasagi *et al*. [17] and Kasagi & Ohtsubo [18] have performed direct numerical simulations of turbulent channel flows with $Re_\tau = 150$ and Prandtl numbers of 0.71 and 0.025, respectively. In these cases the iso-flux boundary condition is applied on the two walls so that the local mean temperature increases linearly in the streamwise direction. Detailed budgets for the scalar variance, its dissipation rate and the scalar fluxes are presented in these cases.

In the channel-flow DNS of Kawamura *et al*. [19] Re_τ is 180 and Prandtl numbers in the range 0.025-5 are studied. In that of Kawamura & Abe [20] Re_τ is 180 and 395 and Prandtl numbers of 0.025, 0.2 and 0.71 are used. Also in these studies the iso-flux boundary condition is applied and detailed budgets for the scalar variance, its dissipation rate and the scalar fluxes are presented. A Prandtl number of 5 and a Reynolds number Re_τ of 395 are the highest values for which data have been published. The numerical method used by Kawamura *et al*. and Kawamura & Abe is a finite-difference method, whereas Kim & Moin [22], Kasagi *et al*. [17] and Kasagi & Ohtsubo [18] use spectral methods. Spectral methods have a higher accuracy than finite-difference methods, whereas the latter have the advantage of being more easily applied to complex geometries.

4.1. Numerical method

The numerical code used for the direct numerical simulation presented in this thesis is based on the channel-flow code of Lundbladh *et al*. [26], which has been extended to also compute the evolution of a passive scalar field. It is similar to that of Kim & Moin [22], Kasagi *et al.* [17] and Kasagi & Ohtsubo [18]. The present simulation code uses spectral methods, with Fourier representation in the streamwise (x) and spanwise (z) directions, and Chebyshev polynomials in the wall-normal (y) direction. Time integration is carried out using the Crank-Nicolson scheme for viscous terms and a four-stage Runge-Kutta scheme for the nonlinear terms.

The equations that are solved for the velocity field are the normal velocity equation and the normal vorticity equation. It is sufficient to calculate these two components since the other velocity components may be obtained from the incompressibility constraint and from the definition of the normal vorticity. Using this solution procedure the pressure is eliminated from the equations and the number of variables to be solved for is reduced from four to two. Including the passive scalar, the total number of variables that are solved for are thus three.

The equation for the total normal vorticity field is given by

$$\frac{\partial \omega}{\partial t} = h_\omega + \frac{1}{Re}\frac{\partial^2 \omega}{\partial x_l \partial x_l} \tag{25}$$

and that for the total scalar field is

$$\frac{\partial \Theta'}{\partial t} = h_\theta + \frac{1}{Pr Re}\frac{\partial^2 \Theta'}{\partial x_l \partial x_l}. \tag{26}$$

These equations are identical except for the nonlinear terms h_ω and h_θ, and the molecular Prandtl number (or Schmidt number) appearing in (26). The nonlinear term h_θ is given by

$$h_\theta = -U'_l \frac{\partial \Theta'}{\partial x_l} \tag{27}$$

The solution procedure applied to the conservation equation (26) is identical to that of the normal vorticity equation, (25), except for the boundary conditions.

4.2. Numerical procedure

The present direct numerical simulation of a turbulent channel flow with a passive scalar has a friction Reynolds number, Re_τ, of 265, a Reynolds number based on the centerline mean velocity and the channel half width of 4800, and a Prandtl number (or Schmidt number) of 0.71. The simulations were performed on a Cray-J932 using a number of processors in parallel, which significantly reduced the computation time. The present Reynolds number is the highest for which data of a turbulent channel flow with an imposed mean scalar gradient, obtained by using a spectral code, has been reported in the literature. The computational domain is 12.56δ, 2δ, 5.5δ in the streamwise, wall-normal and spanwise directions respectively and the number of grid points is $256\times193\times192$. This gives a resolution in the x-, y- and z-directions of 13.0, 2.7(on average) and 7.6 wall units respectively.

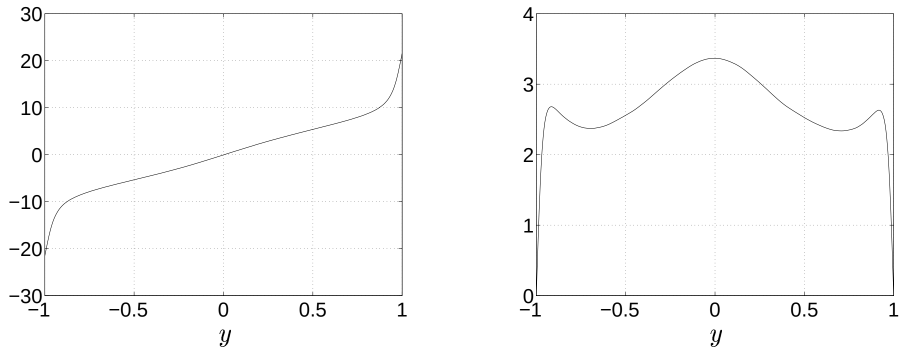

FIGURE 4.1 Left: The mean scalar distribution, Θ^+, in wall units throughout the channel. Right: The *rms* of the fluctuating scalar, $\sqrt{\overline{\theta^{+2}}}$, in wall units throughout the channel.

The passive scalar, *e.g.* temperature, at each wall is kept constant with a higher temperature on the upper wall. This boundary condition represents a case in which the passive scalar is introduced at the upper wall and removed from the lower wall. This type of boundary condition, for which the resulting mean scalar profile in the channel becomes antisymmetric, has also been used by *e.g.* Kim & Moin [22], Na *et al.* [27] and Kawamura (private communication). In Fig. 4.1 the mean scalar profile and the *rms* of the fluctuating scalar are given in wall units throughout the channel. These profiles are quite different from those obtained using the iso-flux boundary condition or those obtained with an internal source term and isothermal walls of equal temperature. In these two latter cases the mean scalar profile is symmetric, giving zero production at the centerline, and the *rms* profile has a local minimum in the center of the channel, *i.e.* a shape more similar to that of the kinetic energy. The local maximum near the wall becomes more pronounced with increasing Prandtl number in the cases studied by *e.g.* Kawamura *et al.* [19] and Kawamura & Abe [20].

4.3. The mean passive scalar profile

Fig. 4.2 shows the dimensionless mean scalar distribution, $\Theta^+ - \Theta^+_{\text{wall}}$, in wall units. For $y^+ < 5$ this is given by $Pr\, y^+$ corresponding to the viscous sublayer profile, $U^+ = y^+$, for the mean velocity. In Fig. 4.3 it is seen that there is a small region in which the slope of $\Theta^+ - \Theta^+_{\text{wall}}$ is constant in the semi-log plot, *i.e*

$$\Theta^+ - \Theta^+_{\text{wall}} = \frac{1}{\kappa_\theta} ln\, y^+ + B_\theta, \tag{28}$$

where κ_θ is the von Kármán constant. The von Kármán constant value, 0.33, is close to values obtained previously by Kasagi *et al.* [17] (0.36 with $Re_\tau = 150$, $Pr = 0.71$) and Kawamura (private communication, about 0.3 with $Re_\tau = 150$, $Pr = 0.71$). Both these previous results were obtained with an iso-flux boundary

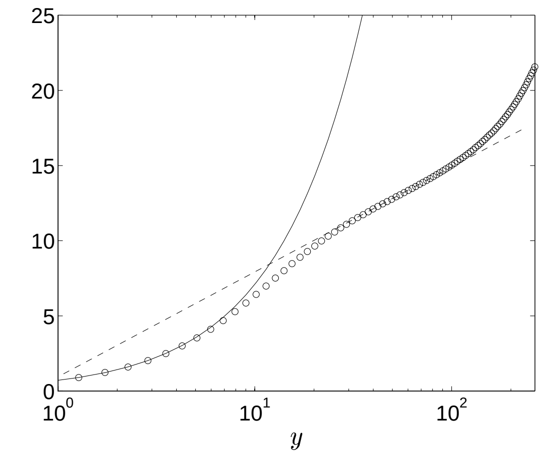

FIGURE 4.2 The dimensionless mean scalar distribution in wall units.
$\circ$, $\Theta^+ - \Theta^+_{\text{wall}}$; —, $Pr\, y^+$; - - -, $3.0 \ln y^+ + 0.95$

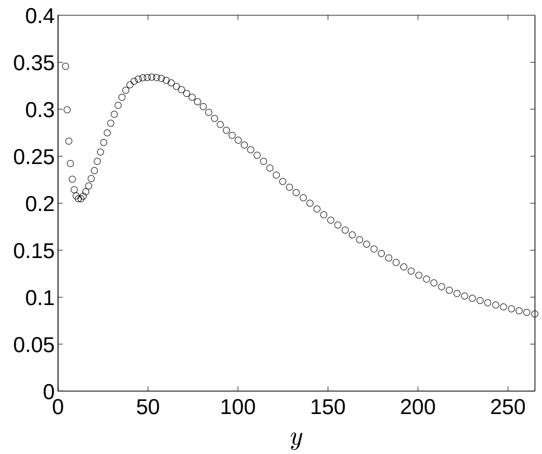

FIGURE 4.3 The von Kármán constant $\kappa_\theta = 1/\frac{\partial \Theta^+}{\partial y^+}\, y^+$.

condition, whereas the isothermal boundary condition is applied here. The κ_θ value should be compared to the velocity-profile related von Kármán constant which is 0.41. The additive constant B_θ is here 0.95. The Nusselt number, given by $Nu = 2h\delta/k$, where h is the heat transfer coefficient and k is the thermal conductivity, is 17.4.

4.4. Results

In Paper 2 the budgets for the scalar fluxes from the present DNS data are presented. For both flux components there is an approximate balance between

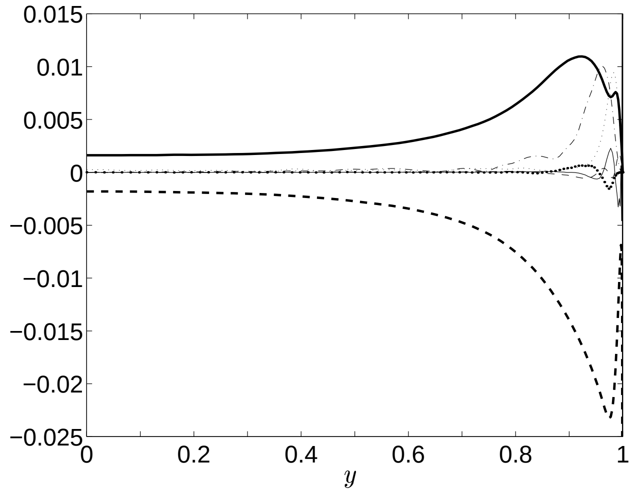

FIGURE 4.4 Terms in the budget of the scalar dissipation rate, ε_θ, in wall units. —, $\alpha \frac{\mathrm{d}^2\varepsilon_\theta}{\mathrm{d}y^2}$; - - -, $-\frac{\mathrm{d}}{\mathrm{d}y}\overline{v\varepsilon'_\theta}$; —, $-2\alpha \overline{\frac{\partial u_j}{\partial x_k}\frac{\partial\theta}{\partial x_k}\frac{\partial\theta}{\partial x_j}}$; · · ·, $-2\alpha \overline{\frac{\partial v}{\partial x_k}\frac{\partial \theta}{\partial x_k}}\frac{\mathrm{d}\Theta}{\mathrm{d}y}$; - · -, $-2\alpha \overline{\frac{\partial\theta}{\partial x}\frac{\partial\theta}{\partial y}}\frac{\mathrm{d}U}{\mathrm{d}y}$; ···, $-2\alpha\,\overline{v\frac{\partial\theta}{\partial y}}\frac{\mathrm{d}^2\Theta}{\mathrm{d}y^2}$; - - -, $-2\alpha^2\overline{\left(\frac{\partial^2\theta}{\partial x_j\partial x_k}\right)^2}$

pressure scalar-gradient correlation and production except in the near-wall region. In the central parts of the channel the destruction is negligible, which was also found to be the case in the DNS of isotropic turbulence with an imposed mean scalar gradient by Overholt & Pope [31], at high enough Reynolds numbers. The budget for the streamwise scalar flux, $\overline{u\theta}$, is very similar throughout the channel to that of Kasagi *et al.* [17], using $Pr = 0.71$ and the iso-flux boundary condition. The budget for the wall-normal scalar flux, $\overline{v\theta}$, is however quite different in the central parts of the channel, since in this region the production, the turbulent diffusion, the pressure scalar-gradient correlation and the pressure diffusion are all non-zero in the present case. In Papers 2 and 3 the modelling of the sum of the pressure scalar-gradient correlation and destruction terms appearing in the Reynolds-flux transport equation is considered using the present DNS data. It is concluded that the pressure scalar-gradient correlation, as in the cylinder wake case, plays an important role in the budget. This data set is also one of the test cases for the explicit algebraic Reynolds-flux model presented in Paper 3 and (more briefly) in Chapter 5, where the scalar fluxes are shown.

In Paper 4 [57] the budgets of the scalar variance, $\overline{\theta^2}$, and the dissipation rate of half the scalar variance, ε_θ, are presented. For the scalar variance budget there is an approximate balance between production and dissipation except in the near-wall region. Both the turbulent diffusion and the molecular diffusion terms are negligible except near the wall. At the wall there is a balance between molecular diffusion and dissipation. This budget is similar to that of Kasagi *et al*. [17], Kawamura *et al*. [19] and Kawamura & Abe [20], except in the center of the channel where the production and dissipation are non-zero for the present case. The difference, between applying the present boundary condition and the iso-flux boundary condition, is thus that the production and dissipation terms do not approach zero as the center of the channel is approached. In Kawamura & Abe [20] it is seen that the production and dissipation terms in this budget both increase for increasing Reynolds numbers.

The present ε_θ budget, presented in Fig. 4.4, is also similar to that of Kasagi *et al*. [17] in the near wall region. In the central parts there is an approximate balance between turbulent (vortex stretching) production and diffusive destruction, whereas the rest of the terms are negligible in comparison with these. For modelling purposes these two are lumped together into a destruction term, which means that in this context the leading order contributions in the budget are essentially cancelled out. As in the scalar variance budget, the production and destruction terms are non zero at the centerline. In Paper 4 the modelling of the transport equation of the scalar dissipation rate is considered using the present DNS data and comparisons are made with the models of Sanders & Gökalp [39] and Yoshisawa [60].

CHAPTER 5

Explicit algebraic scalar-flux modelling

Explicit algebraic scalar-flux models that are derived from second-order closure models have been developed by several investigators previously. These models are attractive since they lead to fewer numerical problems and reduced computational efforts compared to full second-order closures and implicit algebraic models, while they still contain substantially more of the underlying physics than standard two-equation models. Several explicit algebraic scalar-flux models based on the equilibrium assumption for the scalar-flux transport equation, *i.e.* neglect of the advection and diffusion of the scalar flux, have been presented in the literature, see *e.g.* Launder [25] and So *et al.* [45]. In Paper 3 a new explicit algebraic Reynolds-flux model is presented. The modelling approach for the Reynolds fluxes, $\overline{u_i\theta}$, is analogous to that of an EARSM for the Reynolds-stress anisotropy, see *e.g.* Wallin & Johansson, [50] and [51], Gatski & Speziale [13] or Taulbee [46]. The equilibrium hypothesis introduced by Rodi [35] and [36], which is analogous to neglecting the transport of the Reynolds-stress anisotropy is here applied to the normalized scalar flux. Note that this approach is qualitatively different from that used by *e.g.* Launder [25] and So *et al* [45], since here the advection and diffusion of the normalized scalar flux are neglected instead of those of the scalar flux itself. This approach for explicit algebraic scalar-flux modelling has been used earlier by *e.g* Adumitroaie *et al.* [3], Abe *et al.* [2] and Girimaji *et al.* [14]. In the model of Rogers *et al.* [38], where homogeneous shear is considered the rate of change of the normalized scalar flux is assumed to be zero.

5.1. The equilibrium assumption

In analogy with the anisotropy tensor the normalized scalar-flux vector

$$\xi_i \equiv \frac{\overline{u_i\theta}}{\sqrt{KK_\theta}} \tag{29}$$

is introduced. As in explicit algebraic Reynolds-stress modelling, where the transport equation for the anisotropy tensor is modelled, an algebraic relation for ξ_i is formed by modelling its transport equation, given by

$$\frac{\mathrm{D}\xi_i}{\mathrm{Dt}} - D_i^{(\xi)} = -\frac{1}{2}\xi_i\left(\frac{\mathcal{P}_\theta - \varepsilon_\theta}{K_\theta} + \frac{\mathcal{P}_K - \varepsilon}{K}\right) + \frac{\mathcal{P}_{\theta i} - \varepsilon_{\theta i} + \Pi_{\theta i}}{\sqrt{KK_\theta}}. \tag{30}$$

The quantities $\mathcal{P}_{\theta i}$, $\varepsilon_{\theta i}$ and $\Pi_{\theta i}$ are the production, destruction and pressure scalar-gradient correlations terms, respectively, in the transport equation, (11), for the scalar fluxes, whereas $D_i^{(\xi)}$ is the diffusion of the normalized scalar flux. In nearly homogeneous steady flows the advection and diffusion of the normalized scalar flux may be neglected, see *e.g.* Adumitroaie *et al.* [3], Abe *et al.* [2] and Girimaji *et al.* [14]. This is a reasonable approximation in many engineering flows especially if the driving forces (the velocity and scalar gradients) are large. In the DNS of homogeneous turbulence with imposed scalar gradients in each of three orthogonal directions, by Rogers *et al.* [37], the normalized Reynolds fluxes reach approximately constant values as time evolves. This is not the case for the (dimensional) scalar fluxes. Since there is no advection and diffusion this thus means that the left hand side of (30) is approximately zero in this homogeneous shear-flow case.

In Figs. 5.1–5.2 the validity of the equilibrium assumption, in the present channel flow, is illustrated. According to this assumption the sum of all the terms on the right-hand side of (30), that is $\frac{\mathrm{D}\xi_i}{\mathrm{Dt}} - D_i^{(\xi)}$ should vanish, *i.e.*, be negligible in comparison with characteristic magnitudes of individual terms on the right-hand side. Since the advective terms, $\frac{\mathrm{D}\xi_i}{\mathrm{Dt}}$, are zero in the channel flow the sum of all the terms on the right hand side of (30) is given by $-D_i^{(\xi)}$. For the ξ_1-component the equilibrium assumption is appropriate except near the wall. This is also the case for the ξ_2-component except in the center of the channel where $D_2^{(\xi)}$ may be said to be non-negligible.

In Paper 3 the equilibrium assumption is shown to be approximately valid also in the major part of the heated cylinder wake. The relative magnitude of the terms neglected in the equilibrium assumption are somewhat larger in this case than in the channel case. In the outer part (for $\eta > 2$) there is a large deviation from equilibrium, but since the scalar fluxes approach zero for $\eta > 2$ this is actually of minor importance.

By applying the equilibrium assumption the following system of algebraic equations is obtained

$$\frac{1}{2}\xi_i\left(\frac{\mathcal{P}_\theta - \varepsilon_\theta}{K_\theta} + \frac{\mathcal{P}_K - \varepsilon}{K}\right) = \frac{\mathcal{P}_{\theta i} - \varepsilon_{\theta i} + \Pi_{\theta i}}{\sqrt{KK_\theta}}, \tag{31}$$

where $\Pi_{\theta i}$ and $\varepsilon_{\theta i}$ need to be modelled. The modelling of these terms is investigated in Papers 1, 2 and 3. Even for models of $\Pi_{\theta i} - \varepsilon_{\theta i}$ that are linear in the scalar flux vector, the resulting algebraic relation (31) will contain a non-linearity due to the fact that the production term, $\mathcal{P}_\theta = -\overline{u_i\theta}\frac{\partial\Theta}{\partial x_i}$, contains the scalar flux. A method for solving this implicit relation in a fully explicit form is proposed in Paper 3, where the scalar production to dissipation ratio is considered and solved for separately. The equation for the scalar production to dissipation ratio is in the general case, studied in Paper 3, a fourth-order equation in three-dimensional mean flows and a cubic equation in two-dimensional mean flows.

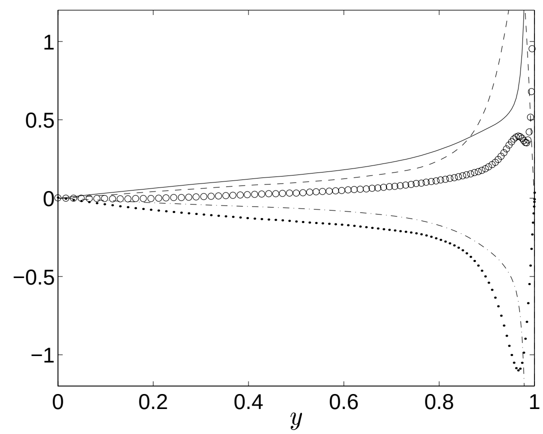

FIGURE 5.1 Validity of the equilibrium assumption for ξ_1 in the channel flow. - - -, $-\xi_1\left(\frac{\mathcal{P}_\theta}{2K_\theta}+\frac{\mathcal{P}_K}{2K}\right)$; - · -, $\xi_1\left(\frac{\varepsilon_\theta}{2K_\theta}+\frac{\varepsilon}{2K}\right)$; ·, $\frac{\mathcal{P}_{\theta 1}}{\sqrt{KK_\theta}}$; —, $\frac{\Pi_{\theta 1}-\varepsilon_{\theta 1}}{\sqrt{KK_\theta}}$; ∘, the sum

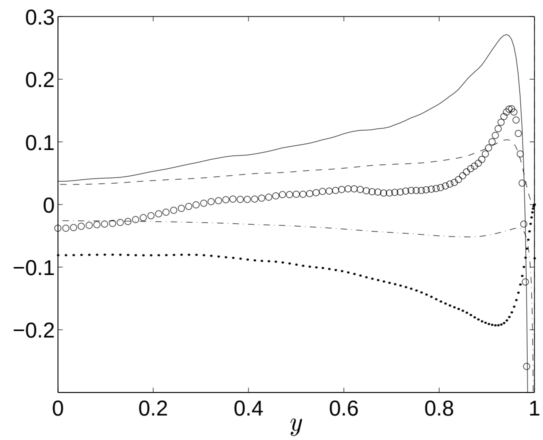

FIGURE 5.2 Validity of the equilibrium assumption for ξ_2 in the channel flow. - - -, $-\xi_2\left(\frac{\mathcal{P}_\theta}{2K_\theta}+\frac{\mathcal{P}_K}{2K}\right)$; - · -, $\xi_2\left(\frac{\varepsilon_\theta}{2K_\theta}+\frac{\varepsilon}{2K}\right)$; ·, $\frac{\mathcal{P}_{\theta 2}}{\sqrt{KK_\theta}}$; —, $\frac{\Pi_{\theta 2}-\varepsilon_{\theta 2}}{\sqrt{KK_\theta}}$; ∘, the sum

The non-linearity, in the algebraic equations for the normalized scalar fluxes, may be eliminated directly by using a non-linear term in the model of the pressure scalar-gradient correlation and the destruction. This results in a much simpler model for both two- and three-dimensional mean flows. The following model, given by

$$\Pi_{\theta i} - \varepsilon_{\theta i} = -\left(c_{\theta 1}\frac{r+1}{r} - \frac{1}{2}\frac{\mathcal{P}_\theta}{K_\theta}\frac{K}{\varepsilon}\right)\frac{\varepsilon}{K}\overline{u_i\theta}, \tag{32}$$

which is proposed in Paper 3, automatically eliminates the non-linear term in (31). By inserting this into (31) the resulting explicit algebraic model for the normalized scalar flux is given by

$$\xi_i = -c_4' A_{ij}^{-1}\left(a_{jk} + \frac{2}{3}\delta_{jk}\right)\Theta_k, \tag{33}$$

where the second-rank tensor A_{ij}, which is given by (72) in Paper 3, contains the normalized mean strain- and rotation-rate tensors

$$S_{ij} \equiv \frac{1}{2}\frac{K}{\varepsilon}\left(\frac{\partial U_i}{\partial x_j} + \frac{\partial U_j}{\partial x_i}\right) \quad \Omega_{ij} \equiv \frac{1}{2}\frac{K}{\varepsilon}\left(\frac{\partial U_i}{\partial x_j} - \frac{\partial U_j}{\partial x_i}\right) \tag{34}$$

and the timescale ratio r. The quantity $a_{ij} \equiv \frac{\overline{u_i u_j}}{K} - \frac{2}{3}\delta_{ij}$ is the Reynolds-stress anisotropy and Θ_i, defined as

$$\Theta_i \equiv \frac{K}{\varepsilon}\sqrt{\frac{K}{K_\theta}}\frac{\partial\Theta}{\partial x_i}, \tag{35}$$

is the normalized mean temperature gradient.

5.2. Model prediction

In Paper 3 several different models for $\Pi_{\theta i} - \varepsilon_{\theta i}$ are studied and invoked in the relation (31). The timescale-ratio dependence in the linear $c_{\theta 1}$-term is found to be important in order to get good agreement for all the test cases (in Paper 3) with the same model-parameter values. The test cases used are the DNS data of a homogeneous shear flow with imposed mean scalar gradients by Rogers *et al.* [37], the DNS data of a turbulent channel flow with a passive scalar, Paper 2, and the experimental data of a heated cylinder wake, Paper 1. The explicit algebraic scalar-flux model (31)-(32) gives good predictions in all three test cases using $c_{\theta 1} = 1.6$. Good agreement is also obtained when excluding the non-linear term in (32) and using $c_{\theta 1} = 1.2$, but in that case the non-linearity in (31) is not eliminated and an equation for the scalar production to dissipation ratio has to be solved. The model (31)-(32) is strongly recommended since it gives both good predictions and a simple formulation.

TABLE 1 The predictions of the scalar fluxes of the model (31),(32) compared to the DNS data of Rogers et al. [37], case C128U, Pr=0.71, at St=12. Case 1: Scalar gradient in the streamwise direction, Case 2: Scalar gradient in the cross-stream direction.

	$\overline{u\theta}$, Case 1	$\overline{v\theta}$, Case 1	$\overline{u\theta}$, Case 2	$\overline{v\theta}$, Case 2
DNS data	−2.41	0.45	0.94	−0.36
(31),(32)	−2.05	0.42	1.13	−0.46

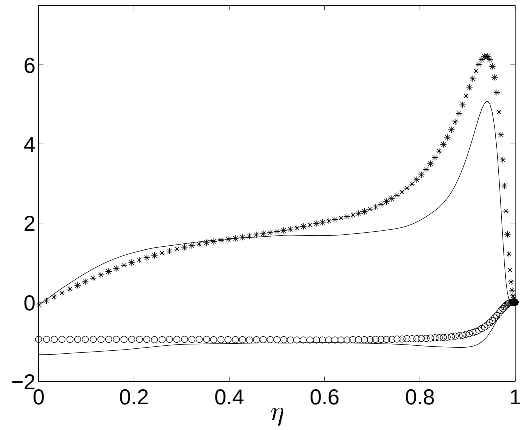

FIGURE 5.3 Model predictions of the scalar flux components in the channel flow. —, model (31),(32); $*$, $-\overline{u\theta}$ from DNS; $\circ$, $\overline{v\theta}$ from DNS.

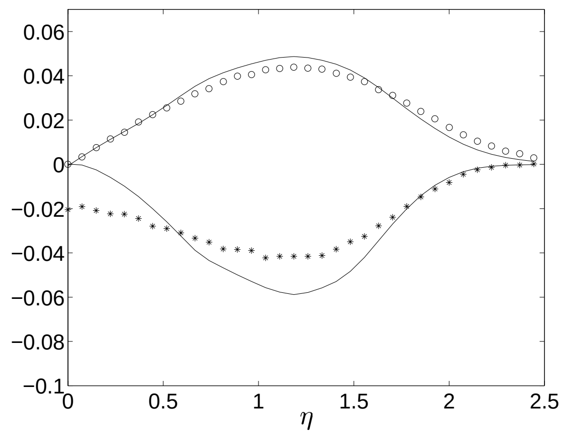

FIGURE 5.4 Model predictions of the scalar flux components in the cylinder wake. —, model (31),(32); $*$, $\overline{u\theta}$ from experiments; $\circ$, $\overline{v\theta}$ from experiments.

In Table 1 and Figs. 5.3-5.4 the model predictions of (31)-(32) are shown for the different test cases. It is seen that good predictions of both components in all three test cases are obtained using the same value of the one and only model parameter, $c_{\theta 1}$. These predictions should be compared to those of an eddy-diffusivity hypothesis, given by (22), for which the prediction of the scalar-flux vector is aligned with the mean scalar gradient. In the channel flow, the heated cylinder wake, and in Case 1 for the homogeneous shear flow, the streamwise scalar flux component, $\overline{u\theta}$, is then predicted to be zero.

CHAPTER 6

Concluding remarks

In the study of the spreading of passive scalars in turbulent flows we have combined physical (Papers 1,5) and numerical (Papers 2,4) experiments of 'canonical' flow cases to extract and analyze features of importance for the mathematical modelling of passive scalar transport. In the experiments on the heated cylinder wake and in the direct numerical simulations (using spectral methods) of turbulent channel flow the Reynolds numbers were higher than in previously reported studies. In both cases budgets for the scalar variance and flux vector could be analyzed from the data. These results together with earlier published data on homogeneous shear flow with imposed mean scalar gradients served as a basis in the development of a new explicit algebraic scalar-flux model (Paper 3) that was shown to yield attractively simple expressions in both two- and three-dimensional mean flows. For practical computations the explicit algebraic scalar-flux model has to be complemented by modelled transport equations for the scalar variance and its dissipation rate. These modelling aspects are analyzed (Paper 4) and tested against the DNS data for the present channel flow.

A remaining issue is that of near-wall treatment and the corresponding need for damping functions in the model. This is left outside the scope of the present thesis and resembles in nature the corresponding issue for explicit algebraic Reynolds-stress models (see Wallin & Johansson [50] and [51]).

The eddy-diffusivity models used in most industrial codes could easily be modified to include the proposed explicit algebraic scalar flux model. This would introduce much more of the underlying physics into the modelling without involving a significant increase in the computational effort.

Acknowledgments

I wish to thank my supervisor Arne Johansson who with his great knowledge in the field of turbulence inspired me to become a turbulence researcher. Arne has lead me through my studies with encouragement and professionalism, which has developed me into an independent self-confident turbulence explorer. I also wish to thank Arne and Anthony Burden for reading earlier versions of this thesis.

I want to thank Magnus Hallbäck and Torbjörn Sjögren who both with great enthusiasm introduced me into my experimental studies.

My cooperation with Stefan Wallin has been very inspiring with many fruitful discussions in the field of turbulence modelling. Dedication together with a large amount of humor made our work together very pleasant.

I would really like to thank all my colleges, friends and room mates at the Department of Mechanics for providing a very stimulating and professional atmosphere to work in.

Above all I wish to thank my dear mother for all her love and support.

The financial support from the Göran Gustafsson Foundation and Ernst Johnsson Foundation (first year) is gratefully acknowledged.

Bibliography

[1] Abe, K., Kondoh, T. & Nagano, Y. 1995 'A new turbulence model for predicting fluid flow and heat transfer in separating and reattatching flows–II'. *Int. J. Heat Mass Transfer* **38**, 1467-1481.

[2] Abe, K., Kondoh, T. & Nagano, Y. 1996 'A two-equation heat transfer model reflecting second-moment closures for wall and free turbulent flows'. *Int. J. Heat and Fluid Flow* **17**, 228-237.

[3] Adumitroaie, V., Taulbee, D. B. & Givi, P. 1997 'Explicit algebraic scalar-flux models for turbulent reacting flows'. *A. i. ch. e. J.* **8**, 1935-2147.

[4] Antonia, R. A. & Browne, L. W. B. 1986 'Anisotropy of temperature dissipation in a turbulent wake'. *J. Fluid Mech.* **163**, 393-403.

[5] Aronson, D. & Löfdahl, L. 1993 'The plane wake of a cylinder: Measurements and interferences on turbulence modeling'. *Phys. Fluids A.* **5**, 1433-1437.

[6] Browne, L. W. B. & Antonia, R. A. 1986 'Reynolds shear stress and heat flux measurements in a cylinder wake'. *Phys. Fluids A.* **29**, 709-713.

[7] Corrsin, S. 1952 'Heat transfer in isotropic turbulence'. *J. Appl. Phys.* **23**, 113-118.

[8] Craft, T. J. & Launder, B. E., 1989 'A new model for the pressure/scalar-gradient correlation and its application to homogeneous and inhomogeneous free shear flows'. *7:th Symp. on Turbulent Shear Flows*, Stanford University, 17.1.1-17.1.6.

[9] Craft, T. J. & Launder, B. E., 1996 'Recent developments in second-moment closure for buoyancy-affected flows'. *Dynamics of Atmospheres and Oceans* **23**, 99-114.

[10] Daly, B. J. & Harlow, F. H. 1970 'Transport equations in turbulence'. *Int. Phys. Fluids* **13**, 2634-2649.

[11] Fabris, G. 1979, 'Conditional sampling study of the turbulent wake of a cylinder'. *J. Fluid Mech.* **94**, 673-709.

[12] Freymuth, P. & Uberoi, M. S. 1971 'Structure of temperature fluctuations in the turbulent wake behind a heated cylinder'. *Phys. Fluids A.* 14, 2574-2580.

[13] Gatski, T. B. & Speziale, C. G. 1993 'On explicit algebraic stress models for complex turbulent flows'. *J. Fluid Mech.* **254**, 59-78.

[14] Girimaji, S. S. & Balachandar, S. 1998 'Analysis and modeling of buoyancy-generated turbulence using numerical data'. *Int. J. Heat Mass Transfer* **41**, 915-929.

[15] Iacovides, H. 1998 'Computation of flow and heat transfer through rotating ribbed passages'. *International Journal of Heat and Fluid Flow* **19**, 393-400.

[16] von Kármán, T. 1939 'The analogy between fluid friction and heat transfer'. Transactions of the American Society of Mechnical Engineers **61**, 705-710.

[17] Kasagi, N., Tomita Y. & Kuroda, A. 1992 'Direct numerical simulation of passive scalar field in a turbulent channel flow'. Trans. of the ASME, **114**, 598-606.

[18] Kasagi, N. & Ohtsubo, Y. 1993 'Direct numerical simulation of low Prandtl number thermal field in a turbulent channel flow'. *Turbulent Shear Flows 8*, Springer-Verlag, Berlin, 97-119.

[19] Kawamura, H., Ohsaka, K., Abe, H. & Yamamoto, K. 1998 'DNS of turbulent heat transfer in channel flow with low to medium-high Prandtl number fluid'. *International Journal of Heat and Fluid Flow* **19**, 482-491.

[20] Kawamura, H. & Abe, H. 1998 'DNS of turbulent heat transfer in channel flow with respect to Reynolds-number effect'. In Proc. of *Turbulent Heat Transfer II*, pp. 1-15–1-22, May 31-June 5, Manchester.

[21] Kim, J., Moin, P. & Moser, R. 1987 'Turbulence statistics in fully developed channel flow'. *J. Fluid Mech.* **177**, 133-166.

[22] Kim, J. & Moin, P. 1989 'Transport of passive scalars in a turbulent channel flow'. *Turbulent Shear Flows 6*, Springer-Verlag, Berlin, 85-96.

[23] LaRue, J. C. & Libby, P. A. 1974 'Temperature and intermittency in the turbulent wake of a heated cylinder'. *Phys. Fluids* **17**, 873-878.

[24] Launder, B. E. 1975 'On effects of a gravitational field on the turbulent transport of heat and momentum'. *J. Fluid Mech.* **67**, 569-581.

[25] Launder, B. E. 1978 'Heat and mass transport.' In *Turbulence* (ed. P. Bradshaw), Topics in Applied Physics **12** 231-287, Springer.

[26] Lundbladh, A., Henningson, D. S. & Johansson, A. V. 1992 'An efficient spectral integration method for the solution of the Navier-Stokes equations'. FFA-TN 1992-28, Aeronautical Research Institute of Sweden, Bromma.

[27] Na, Y., Papavassiliou, D. V. & Hanratty, T. J. 1998 'Use of direct numerical simulation to study the effect of Prandtl number on temperature fields'. *Turbulent Heat Transfer II*, 1-3–1-14, May 31-June 5, Manchester.

[28] Nagano, Y. & Kim, C. 1988 'A two-equation model for heat transport in wall turbulent shear flows'. *J. of Heat Transfer* **110** 583-589.

[29] Nagano, Y., Tagawa, M. & Tsuji, T . 1991 'An improved two-equation heat-transfer model for wall turbulent shear flows'. In Proc. of the *ASME/JSME Thermal Engineering Joint Conference*, Vol. 3, pp. 233-24, J. Lloyd and Y. Kurosaki (eds.), ASME, New York.

[30] Newman, G. R., Launder, B. E. & Lumley, J. L. 1981 'Modelling the behaviour of homogeneous scalar turbulence'. *J. Fluid Mech.* **111**, 217-232.

[31] Overholt, M. R. & Pope S. B. 1996 'Direct numerical simulation of a passive scalar with imposed mean scalar gradient in isotropic turbulence'. *Phys. of Fluids* **8**, 3128-3148.

[32] Prandtl, L. *Z. Physik* **11**, 1072.

[33] Reynolds, O. 1874 'On the extent and action of the heating surface for steam boilers'. *Proceedings of the Manchester Literary and Philosophical Society.* **14**, 7-12.

[34] Reynolds, O. 1883 'An experimental investigation of the circumstances which determine whether the motion of water shall be direct or sinuous, and of the law of resistance in parallel channels'. *Phil. Trans. Roy. Soc.* **174**, 935-982.

[35] Rodi, W. 1972 'The prediction of free turbulent boundary layers by use of a two equation model of turbulence'. *Ph.D. thesis, University of London*

[36] Rodi, W. 1976 'A new algebraic relation for calculating the Reynolds stresses'. *Z angew. Math. Mech.* **56**, T219-221.

[37] Rogers, M., Moin P. & Reynolds, W. 1986 'The structure and modeling of the hydrodynamic and passive scalar fields in homogeneous turbulent shear flow'. Dept. Mech. Engng. Rep. TF-25, Stanford University, Stanford, California.

[38] Rogers, M. M., Mansour, N. N. & Reynolds, W. C. 1989 'An algebraic model for the turbulent flux of a passive scalar', *J. Fluid Mech.* **203**, 77-101.

[39] Sanders, J. P. H. & Gökalp, I. 1998 'Scalar dissipation rate modelling in variable density turbulent axisymmetric jets and diffusion flames'. *Phys. of Fluids* **10**, 938-948.

[40] Shabany, Y. & Durbin, P. A. 1997 'Explicit algebraic scalar flux approximation'. *AIAA J.* **35**, 985-989.

[41] Shih, T. H. 1996 'Constitutive relations and realizability of single-point turbulence closures'. Turbulence and Transition Modelling, Hallbäck et al. (eds), Vol 2.

[42] Shih, T. H. & Lumley, J. L. 1993 'Remarks on turbulent constitutive relations'. *Mathl. Comput. Modelling* **18**(2), 9-16.

[43] Sirivat, A. & Warhaft, Z. 1983 'The effect of a passive cross-stream temperature gradient on the evolution of temperature variance and heat flux in grid turbulence'. *J. Fluid Mech.* **128**, 323-346.

[44] So, R. M. C., Yuan, S. P. & Sommer, T. P. 1992 'A hierarchy of near-wall closures for turbulent heat-transfer'. *Trends Heat Mass Momentum Transfer* **2**, 203-221.

[45] So, R. M. C. & Sommer, T. P. 1996 'An explicit algebraic heat-flux model for the temperature field'. *Int. J. Heat Mass Transfer* **39** no.3, 455-465.

[46] Taulbee, T. B. 1992 'An improved algebraic Reynolds stress model and corresponding nonlinear stress model'. *Phys. Fluids A* **4**, 2555-2561.

[47] Tavoularis, S. & Corrsin, S. 1981 'Experiments in nearly homogeneous turbulent shear flow with a uniform mean temperature gradient'. *J. Fluid Mech.* **104**, 311-367.

[48] Taylor, G. I. 1932 'The transport of vorticity and heat through fluids in turbulent motion'. *Proceedings of the Royal Society*, A, vol. cxxxv, 685-705.

[49] Townsend, A. A. 1949, *Australian J. Sci. Res.*, **2**, 451.

[50] Wallin, S. & Johansson, A. V. 1996 'A complete explicit algebraic Reynolds stress turbulence model including an improved near-wall treatment'. In Proc. of *Flow Modeling and Turbulence Measurements VI*, pp. 399-406, Tallahassee FL, Chen *et al.* (eds.), Balkema.

[51] Wallin, S. & Johansson, A. V. 1997 'A complete explicit algebraic Reynolds stress model for incompressible and compressible turbulent flows'. FFA TN 1997-51, submitted to J. Fluid Mech.

[52] Warhaft, Z. & Lumley, J. L. 1978 'An experimental study of decay of temperature fluctuations in grid-generated turbulence'. *J. Fluid. Mech.* **88**, 659-685.

[53] Wikström, P. M., Hallbäck, M. & Johansson, A. V. 1996 'Measurements and modeling of temperature fluctuations in a heated cylinder wake'. In Proc. of *Flow Modeling and Turbulence Measurements VI.*, pp. 143–150, Tallahassee FL, Chen *et al.*, (eds.), Balkema.

[54] Wikström, P. M., Hallbäck, M. & Johansson A. V. 1998 'Measurements and heat-flux transport modelling in a heated cylinder wake'. *International Journal of Heat and Fluid Flow* **19**, 556-562.

[55] Wikström, P. M. & Johansson, A. V. 1998 'DNS and scalar-flux transport modelling in a turbulent channel flow'. In Proc. of *Turbulent Heat Transfer II*, pp. 6-46–6-51, May 31-June 5, Manchester, UK.

[56] Wikström, P. M., Wallin S. & Johansson, A. V. 1998 'Derivation and investigation of a new explicit algebraic model for the passive scalar flux'. Submitted for publication.

[57] Wikström, P. M. & Johansson, A. V. 1998 'On the modelling of the transport equation for the passive scalar flux'. *4th International Symposium on Engineering Turbulence Modelling and Measurements*, May 24-26 1999, Corsica, France.

[58] Wikström, P. M. 1998 'Velocity and temperature measurements in the self-preserving region of a heated cylinder wake'. TRITA-MEK, Technical Report 1998:9, Dept. of Mechanics, KTH, Stockholm, Sweden.

[59] Youssef, M. S., Nagano, Y, & Tagawa, M. 1992 'A two-equation heat transfer model for predicting turbulent thermal fields under arbitrary wall thermal conditions'. *Int. J. Mass Transfer* **35**, 3095-3104.

[60] Yoshizawa, A. 1988 'Statistical modelling of passive-scalar diffusion in turbulent shear flows'. *J. Fluid. Mech.* **195**, 541-555.